

*Original Article***Development of a stiffness measurement system and biomechanical model of ankle joint to evaluate viscoelasticity and muscle contraction**Yutaka Tomita, RE, PhD,<sup>1</sup> Genichi Tanino, RPT,<sup>1,2,3</sup> Shiho Mizuno, MD, PhD,<sup>2,3</sup>Hirofumi Maeda, MD,<sup>2,3</sup> Hiroyuki Miyasaka, OTR, PhD,<sup>1,2</sup> Orand Abbas, RE, PhD,<sup>1</sup>Kotaro Takeda, RE, PhD,<sup>1</sup> Shigeru Sonoda, MD, PhD<sup>1,2,3</sup><sup>1</sup>Fujita Memorial Nanakuri Institute, Fujita Health University, Tsu, Mie, Japan<sup>2</sup>Fujita Health University Nanakuri Sanatorium, Tsu, Mie, Japan<sup>3</sup>Department of Rehabilitation Medicine II, School of Medicine, Fujita Health university, Tsu, Mie, Japan**ABSTRACT**

Tomita Y, Tanino G, Mizuno S, Maeda H, Miyasaka H, Orand A, Takeda K, Sonoda S. Development of stiffness measurement system and biomechanical model of ankle joint to estimate viscoelastic and muscle contraction. *Jpn J Compr Rehabil Sci* 2014; 5: 147–155.

**Objective:** This research aimed to develop a system to measure the stiffness of the ankle joint for evaluating spasticity or contracture, and for quantifying the characteristics of spasticity. Functionality of the system was verified by testing it on an able-bodied individual and a hemiplegic patient. Additionally, a biomechanical model was developed to estimate the plantar flexion torque caused by viscoelasticity and muscle contraction.

**Methods:** An electromotor, rack and pinion, potentiometer, and torque sensor were installed on a double Klenzak ankle-foot orthosis (AFO). By rotating the electromotor, the ankle joint of the AFO moves dorsally at a fixed speed. The angle and torque of dorsiflexion were measured simultaneously. The subjects sat either in a chair or a wheelchair and wore the abovementioned AFO in the knee-extension and knee-flexion positions, while the AFO moved dorsally. Electromyograms of the tibialis anterior and gastrocnemius muscles were recorded concurrently. The contributions of elastic, viscous, and muscle-contraction components to the plantar flexion torque

were calculated using the system identification approach.

**Results:** The system's ability to measure dynamic characteristics, and also its accuracy, were confirmed. The plantar flexion torque was found to be larger in the knee-extension position than in the knee-flexion position in both the able-bodied person and the patient. Moreover, the patient showed larger plantar flexion torque than the able-bodied subject.

**Conclusions:** A system that measures ankle-joint stiffness for evaluating spasticity was developed, and sufficient functionality was verified by applying it to both an able-bodied individual and a hemiplegic patient. In addition, plantar flexion torque caused by viscoelasticity and muscle contraction was estimated.

**Key words:** joint stiffness, quantification, viscoelasticity, electromyogram, spasticity

**Introduction**

Measurement of ankle-joint stiffness is indispensable in evaluating the efficacy of treatments for spasticity, which include antispastic medications or nerve blocks using phenol and botulinum toxin type A (BTX-A). Hypertonic muscles, also referred to as spastic muscles, exhibit small resistance torque when they are moved slowly and large resistance torque when they are moved quickly [1]. In order to quantitatively evaluate muscle tone, several methods have been introduced, e.g., the Modified Ashworth Scale and the Tardieu Scale. However, although they are handy and easy to use in clinical situations, these methods have deficiencies such as low interclass correlation coefficients [2, 3]. Quantitative evaluation can be performed using an isokinetic machine such as the Biodex. However, this machine has several drawbacks such as its bulkiness, a high seating position that makes it difficult to transfer a patient from a wheelchair

Correspondence: Yutaka Tomita, RE, PhD

Fujita Memorial Nanakuri Institute, Fujita Health University, 423, Oodori-Cho, Tsu, Mie 514-1296, Japan.

E-mail: tomita@fujita-hu.ac.jp

Accepted: December 7, 2014

No benefits in any form have been or will be received from a commercial party related directly or indirectly to the subject of this manuscript.

to the seat, and the machine's design for active movement measurement, which yields large measurement errors in passive movement torque because it is much smaller than in active movement. Therefore, the machine is only suitable for research purposes and not for clinical application.

We have developed an ankle-joint stiffness measuring system for clinical applications. The system can measure plantar flexion torque under passive dorsiflexion at a constant angular velocity. This system was tested on both an able-bodied individual and a hemiplegic patient to measure ankle-joint plantar flexion stiffness. Moreover, we developed a method to decompose the plantar flexion torque into three components: the torque caused by elasticity, the torque caused by the viscosity of the muscles and soft tissue around the joint, and the torque caused by the contraction of the muscles.

## Methods

### 1. System equipment

The system's equipment consists of an ankle-foot orthosis (AFO) that can move the ankle joint dorsally at a constant angular velocity, a control unit that directs the movement of the AFO, and a two-channel electromyograph. The AFO can be moved by an electromotor (RZ-8BAWA-AWG235X28, Mabuchi Motor, Japan), which turns a pinion through a universal joint (B6AA, Miyoshi Kikai, Japan) and pulls a rack mounted near the metatarsal-phalanx joint of the fifth toe, converting the rotation to dorsiflexion. The dorsiflexion angle can be measured by a potentiometer (RDC1014A09, Alps Electric, Japan), which is installed on the ankle-joint axis.

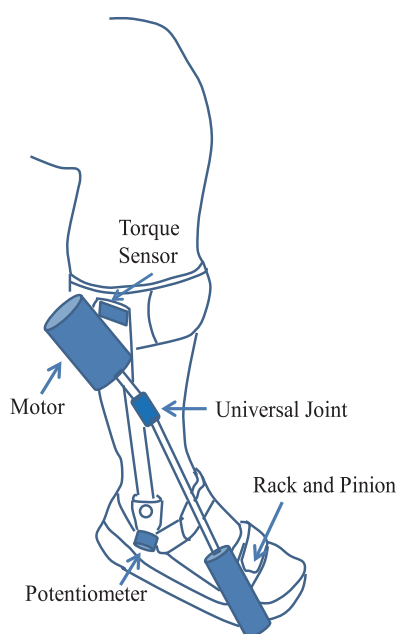


**Figure 1.** Equipment for ankle stiffness measurement.

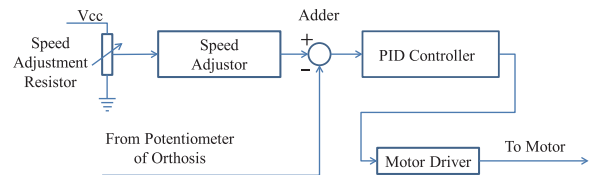


**Figure 2.** Block diagram of control unit.

The torque is measured by strain gauges (KFG-1-120-C1-16, Kyowa Dengyo, Japan) attached to a flange on the AFO, to which an electromotor and a strain amplifier (STA-04G, GeotechService, Japan) are also mounted. The control unit receives a feedback signal from the potentiometer. Using this signal in a proportional-integral-derivative (PID) control mechanism, the foot can be moved dorsally at a constant angular velocity (Figure 2).

Constant angular velocity is achieved in several steps. First, the resistance of the "Speed Adjustment Resistor" is modulated and its values passed to the "Speed Adjustor" to compute the target angle at every moment. The difference between the target angle and the signal of the potentiometer is input to the PID controller, which calculates a proper input signal for the "Motor Driver". Finally, a suitable input voltage for the "Motor Driver" is selected. When the AFO arrives at the target angle, the output of the adder, i.e., the input of the PID controller, is 0 V. The motor driver maintains its output.

The output of the potentiometer and the strain amplifier are transferred to a computer (Sotec WA5512, Intel Core 2 Duo Processor T5500, 1.66 GHz) through a data logger (NR2000, Keyence, Japan) at a sampling rate of 1 kHz. Simultaneously, electromyograms of the tibialis anterior and gastrocnemius muscles are recorded by the data logger after filtering with a second-order Butterworth bandpass filter between 10 and 500 Hz. The ankle joint is passively moved from 20° plantar flexion (-20°) to 10° dorsiflexion (+10°).

### 2. Characteristics of equipment

**Calibration of potentiometer:** Measurement of the potentiometer output voltage and reading of the hand goniometer were performed simultaneously while the ankle-joint angle of the AFO was manually adjusted.

**Calibration of torque sensor:** The AFO was fixed on a table at an upright position (at the 0° angle of plantar and dorsiflexion of the ankle joint), and the calf-band of the orthosis was aligned with the direction of plantar flexion using a spring balance. The strain amplifier and spring balance outputs were simultaneously measured and recorded.

**Setting of angular velocity:** We set several dorsiflexion angular velocities, and calculated the angular velocities from the time-angle plots.

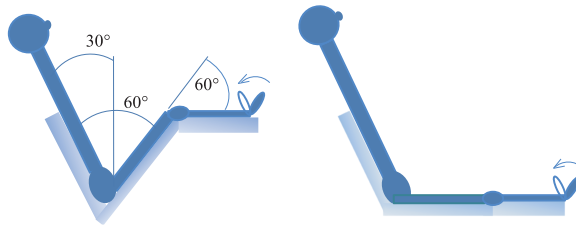


Figure 3. Posture of subject.

### 3. Subjects

The subjects were an able-bodied individual (a female in her fifties) and a constitutional-hemorrhage hemiplegic patient. The latter subject was a right hemiplegic male in his fifties at four months after traumatic brain injury onset. The Stroke Impairment Assessment Set was used as an evaluation battery. The patient's motor functions at the affected side were as follows: 4 in the hip-flexion test, 4 in the knee-extension test, and 3 in the foot-pat test. He was able to walk without a cane or an ankle foot orthosis (Functional Independence Measure was 7). The Modified Ashworth Scale for the group of muscles involved in plantar flexion of the ankle joint was 2.

The subjects sat either on a chair with a back support or in a wheelchair with their back reclined at 30° and their legs positioned on a specially designed support (Figure 3) that bent the body of the femur and lower leg at a 60° angle against the reclined trunk and the body of the femur, respectively. Pairs of electrodes were placed on the tibialis anterior muscle and the gastrocnemius muscle for the electromyogram measurements.

This research and experimental procedure were approved by the local Ethics Committee of Nanakuri Sanatorium, Fujita Health University (approval number 97). Informed consent was obtained from the subjects.

### 4. Viscoelastic model of joint and estimation of its parameters

A viscoelastic model of muscle was proposed by Hill [4] and Winter [5], and improved upon by Phillips [6]. Dell [7] reported a computational model. Figure 4a shows the model by Phillips. It consists of a parallel elastic component and a viscous component, which represent the elasticity and viscosity of muscle, and a serial elastic component that represents the elasticity of tendons. However, because tendons are harder to stretch than muscles, the stiffness of the serial elastic component of this model can be assumed to be

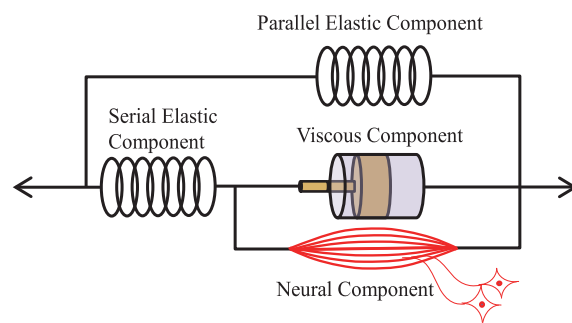


Figure 4a. Muscle model of Phillips's muscle model.

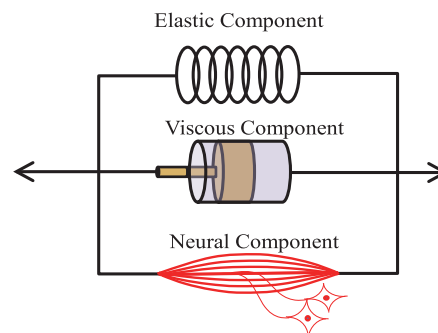


Figure 4b. Voigt of muscle.

Table 1. Nomenclature.

$T_{total}$	: Resistive torque generated by ankle joint
$T_b$	: Resistive passive torque generated by viscous element
$T_k$	: Resistive passive torque generated by elastic element
$T_{AT}$	: Resistive active torque generated by antagonist muscle (Tibialis Anterior)
$T_{AG}$	: Resistive active torque generated by agonist muscle (Gastrocnemius)
$b$	: Coefficient of viscous element
$k$	: Coefficient of elastic element
$\theta$	: Angle of ankle joint
$\dot{\theta}$	: Angular velocity of ankle joint
$EMG_{AG}$	: EMG of agonist muscle
$EMG_{AT}$	: EMG of antagonist muscle
$n_1$	: Coefficient of $EMG_{AG}$
$n_2$	: Coefficient of $EMG_{AT}$
$T$	: Torque vector
$\Omega$	: Input matrix
$\theta$	: Parameter vector

significantly larger than that of the parallel elastic component. Hence, Figure 4a can be approximated by the Voigt model shown in Figure 4b. In this research, because of the simplicity of the model architecture and the ease of parameter estimation, we employed the model of Figure 4b.

The muscles in the investigative model were relaxed and passively plantar flexed. The resultant torque is the sum of the elastic and viscous torque components. Given that these two components are respectively proportional to stretch distance and velocity, their increase results in an increase in the resultant torque. When an ankle joint is slowly dorsiflexed, the work is mainly done by the elastic component. In contrast, when the ankle joint is moved quickly, the viscous component is activated and additionally contributes to the resultant torque. The third component, which contributes to the resultant torque when there is neural activity, is initiated by muscle contraction. This active plantar torque is added to the torque caused by the elastic and viscous components. The model used in the present study considers the biomechanical characteristics of the muscle but not its internal structures. We assumed that the viscoelastic characteristics of joints were also approximated by the same model.

Employing the model of Figure 4b, the measured plantar flexion torque was decomposed into the torque caused by the elastic component  $T_k$  and the viscous component  $T_b$ , and the torque caused by muscle contraction. The muscle contraction torque is the difference in the torque caused by the agonist muscle group,  $T_{AG}$ , and the antagonist muscle group,  $T_{AT}$ , both of which were assumed to be proportional to the absolute values of the corresponding electromyograms ( $EMG_{AG}$  and  $EMG_{AT}$ ).  $T_k$  and  $T_b$  were assumed to be proportional to the dorsiflexion angle  $\theta$  and the angular velocity  $\dot{\theta}$ , respectively. Namely, total plantar flexion torque  $T_{total}$  was derived as follows:

$$T_{total}(t) = T_k(t) + T_b(t) - T_{AT}(t) + T_{AG}(t) + e(t) \\ = k\theta(t) + b\dot{\theta}(t) - n_1(EMG_{AG}(t)) + n_2(EMG_{AT}(t)) + e(t) \quad (1)$$

where  $k$ ,  $b$ ,  $n_1$ , and  $n_2$  are coefficients of the elastic, viscous, agonist, and antagonist components, respectively.  $EMG_{AG}$  and  $EMG_{AT}$  are the root mean squares of the electromyograms (window width of 67 ms) of the agonist and antagonist muscle groups, respectively.  $e(t)$  represents the model error and an error that cannot be explained by Eq. (1).

From the time series of  $\theta$ ,  $T_{total}$ , and the two electromyograms, we defined the following matrix and vectors:

$$\Omega = \begin{bmatrix} \theta(1) & \dot{\theta}(1) - (EMG_{AT}(1)) & (EMG_{AG}(1)) \\ \theta(2) & \dot{\theta}(2) - (EMG_{AT}(2)) & (EMG_{AG}(2)) \\ \vdots & \vdots & \vdots \\ \theta(n) & \dot{\theta}(n) - (EMG_{AT}(n)) & (EMG_{AG}(n)) \end{bmatrix}$$

$$T = \begin{bmatrix} T_{total}(1) \\ T_{total}(2) \\ \vdots \\ T_{total}(n) \end{bmatrix} \\ \theta = \begin{bmatrix} k \\ b \\ n_1 \\ n_2 \end{bmatrix} \\ e = \begin{bmatrix} e(1) \\ e(2) \\ \vdots \\ e(n) \end{bmatrix} \quad (2)$$

Substituting Eq. (2) into Eq. (1), we obtained Eq. (3):

$$T = \Omega\theta + e \quad (3)$$

Given that  $\Omega$  is an  $n \times 4$  matrix, the least squares method can be used to minimize the sum of the squares of  $e(t)$  in Eq. (1), which is equivalent to the inner product of the error term in Eq. (3),  $e^T e$ . The coefficient vector can be obtained as [8]:

$$\theta = (\Omega^T\Omega)^{-1}\Omega^T T \quad (4)$$

where the superscripts T and  $-1$  represent the transposed matrix and the inverse matrix, respectively.

By substituting  $k$ ,  $b$ ,  $n_1$ ,  $n_2$ ,  $\theta(t)$ ,  $\dot{\theta}(t)$ ,  $-(EMG_{AG}(t))$  and  $(EMG_{AT}(t))$  into Eq. (1), we can obtain the total plantar flexion torque.

## Results

### 1. Equipment

**Calibration of potentiometer:** Figure 5 shows the relationship between the ankle-joint angle  $\theta$  (degrees)

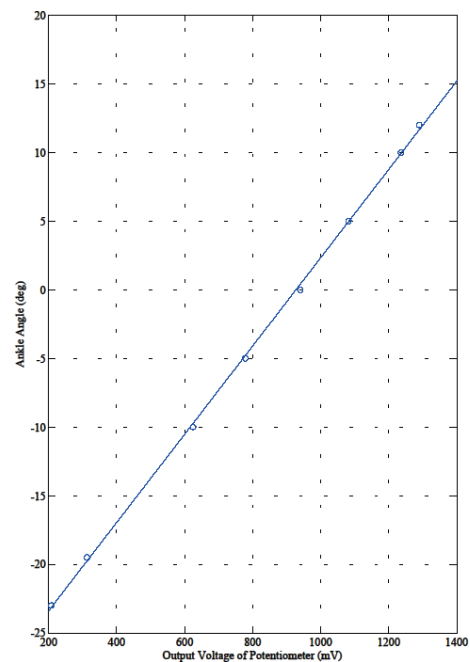


Figure 5. Calibration line of potentiometer.

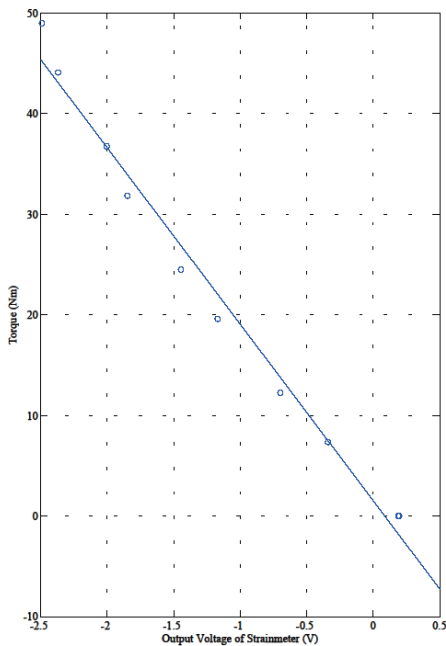


Figure 6. Calibration line of torque sensor.

that was measured using a goniometer and the output of the potentiometer  $V_p$  (V). The following relationship was obtained:

$$\theta = 32.2V_p - 29.82. \tag{5}$$

**Calibration of torque sensor:** The relationship between  $T_{total}$  (Nm), which was measured using a spring balance, and the output of the strain amplifier  $V_s$  (V), is shown in Figure 6, and can be expressed as follows:

$$T_{total} = -17.54V_s + 1.532. \tag{6}$$

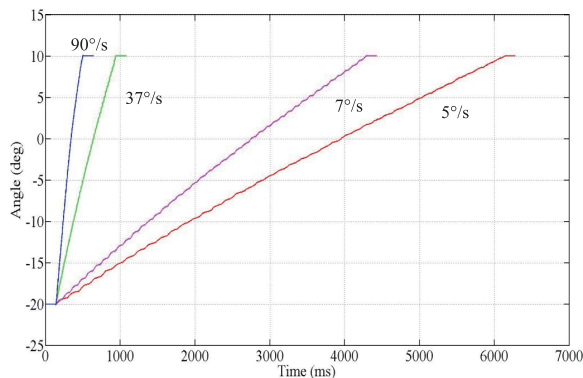


Figure 7. Time course of dorsal flexion angle.

**Setting of angular velocity:** We measured the dorsiflexion angle at various speed settings. The results are shown in Figure 7, where the gradient of the loci are the angular velocities. We verified that the AFO moved at an approximately constant angular velocity.

### 2. Angle-torque curves

The results are shown in Figure 8, where the abscissa is the angle and the ordinate is the torque. Figures 8a to 8d show the analyses of the results of the able-bodied subject and the hemiplegic patient. The blue line is the result at low speed (about 5°/s) and the red line is the result at high speed (about 90°/s). Figures 8a and 8c correspond to cases where the knee joints of the subjects were flexed, and 8b and 8d correspond to cases where their knee joints were extended. Comparing Figures 8a and 8b, the able-

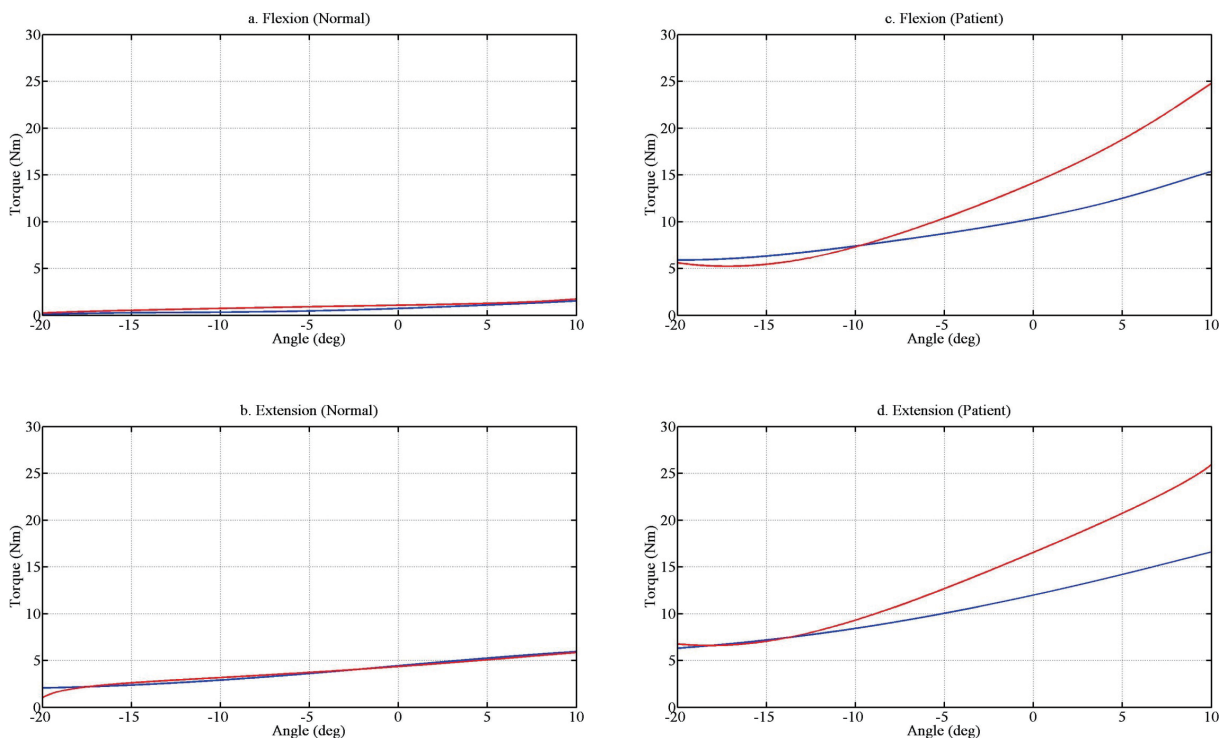
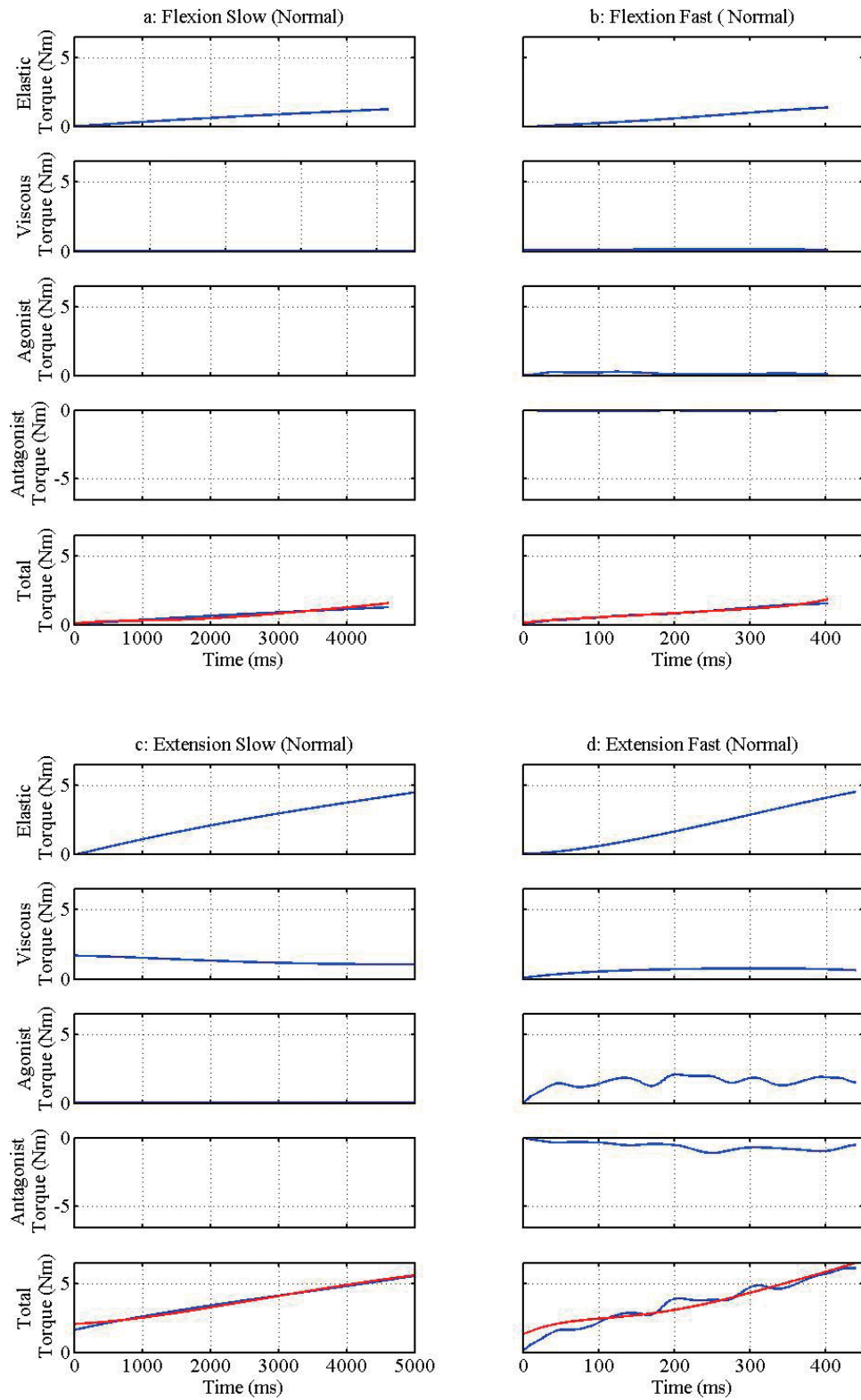
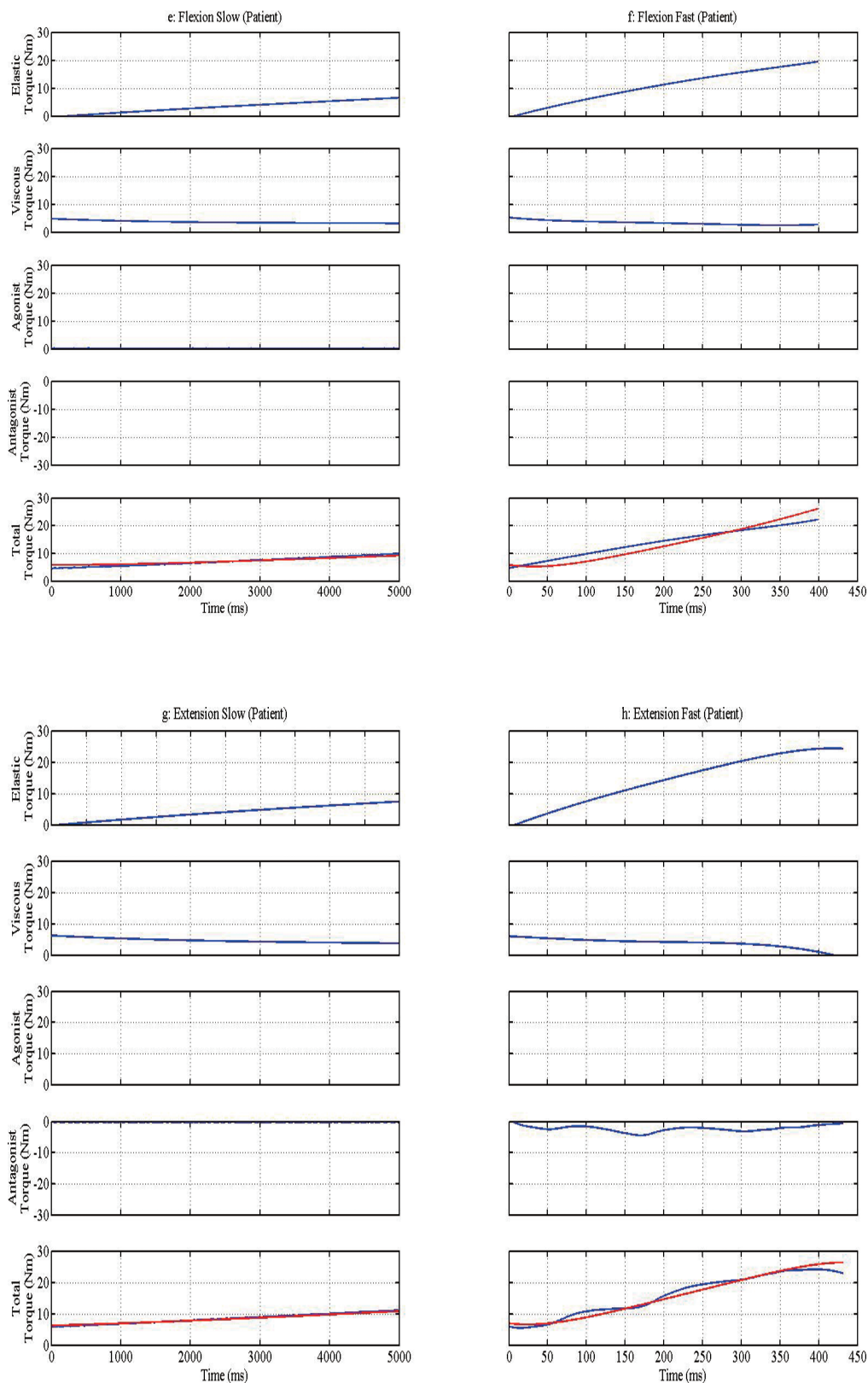


Figure 8. Angle-torque characteristics (blue: slow, red: fast).

a: able-bodied, knee-flexion, b: able-bodied, knee-extension, c: patient, knee-flexion, d: patient, knee-extension.



**Figure 9.** Decomposed torques of each component and sum of them (blue), and measured torque (red).



a: able-bodied, knee-flexion, slow, b: able-bodied, knee-flexion, fast, c: able-bodied, knee-extension, slow, d: able-bodied, knee-extension, fast, e: patient, knee-flexion, slow, f: patient, knee-flexion, fast, g: patient, knee-extension, slow, h: patient, knee-extension, fast.

bodied person showed a larger plantar flexion torque in the knee-extension posture than in the knee-flexion posture. The patient also exhibited the same results.

### 3. Estimation of elastic, viscous, and contracture components

The results of estimating the contribution to plantar flexion torque by the elastic and viscous components, together with the components from the agonist and antagonist muscle groups, are shown in Figures 9a to 9h. The time sequences of the measurement data based on Figure 4b and Eqs.(1) to (4) were used for plantar flexion torque estimation. In the figures, the abscissa is the time (ms) and the ordinate is the plantar flexion torque (Nm). The elastic, viscous, agonist, and antagonist torque is shown in order from top to bottom. The total torque represented by the blue line is shown at the bottom of each figure. The red line on the same subplot represents the measured values. In accordance with our assumption, the torque contributed by the antagonist muscles, which corresponds to dorsiflexion, was negative.

Figure 9a shows the results for the able-bodied person when the knee joint was flexed, with low flexion angular velocity. The elastic component accounts for most of the total torque. Figure 9b shows the results at high flexion angular velocity. The torque caused by the components—elastic, viscous, agonist muscle group, and antagonist muscle group—did not show any remarkable differences. Therefore, the total torque was also not much different from that in Figure 9a.

Figure 9c shows the results for the able-bodied person when the knee joint was extended with slow flexion speed. The plantar flexion torque of the elastic and viscous components became larger compared to that measured in the knee-flexion position (Figures 9a and 9b); however, no muscle activity was observed. Figure 9d shows the results at high flexion angular velocity. Here, in addition to the increase in torque of the elastic and viscous components seen in Figure 9c, activity of the agonist (i.e., gastrocnemius) and antagonist (i.e., tibialis anterior) muscle was observed.

Figure 9e shows the results for the patient when the knee joint was flexed at low flexion angular velocity. The ordinate scale of the torque was five times larger than that of the able-bodied individual. The plantar flexion torque caused by the elastic and viscous components was larger than that of the able-bodied individual. Figure 9f shows the results at high flexion angular velocity. The plantar flexion torque caused by the viscous component did not show a large difference, but the plantar flexion torque caused by the elastic component increased. No muscle contraction contribution was observed. Figure 9g shows the results when the subject's knee joint was extended at low flexion speed. They do not differ from the results shown in Figure 9e. Figure 9h shows the results at high flexion speed. The

plantar flexion torque caused by the elastic component increased while the torque caused by the viscous component and the muscle activity did not differ from the results shown in Figure 9g.

## Discussion

### 1. Characteristic of equipment

As shown in Figures 5 to 7, during the measurement of angle and torque, consistency in the angular velocity was maintained with sufficient accuracy.

### 2. Angle-torque relationship

From Figure 8, we find that the plantar flexion torque with the knee in the extension position is larger than that with the knee in the flexion position for both the able-bodied individual and the patient.

From the posture of the subject shown in Figure 3, it can be seen that the gastrocnemius is not extended while the knee joint is in the flexion position. Therefore, it does not contribute to the measured torque. In the other position, the gastrocnemius is extended and affects the measured torque. This is why the measured torque for the able-bodied individual in Figure 8a and that for the patient in Figure 8c are smaller in comparison to the values in Figures 8b and 8d, respectively.

### 3. Estimation of the elastic, viscous, and contracture components

Given that the estimated torque in Figure 9 agreed well with the measured torque, we conclude that the model shown in Figure 4b properly expresses the biomechanical properties (e.g., stiffness) of the ankle joint.

In the able-bodied individual, we found that the plantar flexion torque did not depend on the dorsiflexion rate, i.e., the torque caused by the elastic and the viscous components did not depend on the rate and muscle contraction did not occur. We also found that in the patient, the torque of the elastic component became large with high-speed dorsiflexion but was not affected by the viscous component.

Moreover, given the small contribution of muscle contraction components to the plantar flexion torque compared with that of the elastic component, it was found that the torque resisting the passive dorsiflexion of the ankle joint of the able-bodied person was not caused by the contracture component of the muscles. It is believed that the plantar flexion torque resisting the passive dorsiflexion of the ankle joint of the patient is not caused by the contracture component of the muscles but by the joint itself (i.e., soft tissues such as the muscle, tendon, joint capsule, etc.) for which the viscoelasticity increases with immobilization. Okita [9] reported similar results. However, we examined only one patient, and without data from more patients, the results cannot be generalized for hemiplegia.

As we used a two-channel EMG, we took the electromyogram measurements of the gastrocnemius muscle as representative of the agonist muscle group. Likewise, the tibialis anterior muscle was taken to be representative of the antagonist muscle group. However, because the soleus muscle may also contribute to the plantar flexion of the ankle joint, the effect of the gastrocnemius muscle and the soleus muscle on the plantar flexion torque cannot be discussed in the present study.

We plan to measure the stiffness of ankle joints from spastic patients both before and after medical treatment to evaluate the effect of the treatments.

We did not attempt to patent the system developed in the present research. We also declare that there are no conflicts of interest.

### References

1. Lance JW. Symposium synopsis. In: Feldman RG, Young RR, Koella WP, editors. Miami, FL, Synopsis Specialists; 1980. pp. 485–9.
2. Bohannon RW, Smith MB. Interrater reliability of a modified Ashworth scale of muscle spasticity. *Phys Ther* 1985; 67: 206–7.
3. Haugh AB, Pandyan AD, Jonson GR. A systematic review of the Tardieu scale for the measurement of spasticity. *Disabil Rehabil* 2006; 28: 899–907.
4. Hill AV. The heat of shortening and the dynamic constants of muscle. *Proc R Soc*: 1938; Ser B126: 136–95.
5. Winters JM. Hill based muscle models: a systems engineering perspective. In: Winters JM, Woo S, editors, *Multiple Muscle Systems: Biomechanics and Movement Organization*, Springer-Verlag, New York; 1990.
6. Phillips CA, Repperger AT, Neidhard-Doll AT, Reynolds DB. Biomimetic model of skeletal muscle isometric contraction: I. an energetic-viscoelastic model for the skeletal muscle isometric force twitch. *Comput Biol Med* 2004; 34: 307–22.
7. Delp SL, Loan JP. A computational framework for simulating and analyzing human and animal movement. *Computing in Science and Engineering - C in S & E* 2000; 2: 46–55.
8. Eykhoff P. System identification-parameter and system estimation, John Wiley & Sons, New York; 1974.
9. Okita M, Nakano J, Kataoka H, Sakamoto J, Origuchi T, Yoshimura T. Effects of therapeutic ultrasound on joint mobility and collagen fibril arrangement in the endomysium of immobilized rat soleus muscle. *Ultrasound Med Biol* 2009; 135: 237–44.